

Article

Effect of Cold Rolling on Recrystallization Behavior of Al-Free and Al-Added 15Cr-ODS Ferritic Steels

Yoosung Ha ^{1,†}  and Akihiko Kimura ^{2,*}¹ Graduate School of Energy Science, Kyoto University, Kyoto 606-8501, Japan; ha.yoosung@jaea.go.jp² Institute of Advanced Energy, Kyoto University, Uji, Kyoto 611-0011, Japan

* Correspondence: kimura@iae.kyoto-u.ac.jp; Tel.: +81-774-38-3476

† Current address: Nuclear Safety Research Center, Japan Atomic Energy Agency, Tokai, Ibaraki 319-1195, Japan.

Received: 26 December 2018; Accepted: 10 March 2019; Published: 12 March 2019



Abstract: The effect of cold rolling on the recrystallization behavior of Al-free and Al-added 15Cr-oxide dispersion strengthened (ODS) ferritic steels was investigated. The recrystallization of both steels are enhanced by cold rolling. The Al-free ODS steel with finer oxide particles is harder to recrystallize than Al-added ODS steel with coarser oxide particles. The effect of Al addition on the recrystallization behavior is evident. It is estimated that the recrystallization temperature of Al-free and Al-added 15Cr-ODS ferritic steel is 900 °C and 1250 °C with the annealing period of 1 h. In Al-free ODS steel, a small hardening was observed in the temperature range between 850 °C and 1200 °C, while no such phenomenon was observed in Al-added ODS steel, which is indicative of retardation of recovery by finely dispersed oxide particles. Oxide particle growth is mostly dependent on annealing temperature, while recrystallization and grain growth are controlled by not only the temperature, but the cold rolling ratio, which alters the multiple factors such as dislocation density, initial grain shape and oxide particle dispersion morphology. The cold rolling direction also influences the grain morphology and grain orientation in Al-added ODS steel, and the second rolling in a perpendicular direction to the first cold rolling direction induces the rotation of the grains from $\langle 110 \rangle$ to $\langle 112 \rangle$. The recrystallization temperature is not significantly changed by the cold rolling direction. Recrystallization after cold rolling appears to increase the $\{111\}$ grain orientation on the cold rolled specimen surface.

Keywords: 15Cr-ODS ferritic steel; recrystallization; cold-rolling; texture; anisotropy

1. Introduction

Oxide dispersion strengthened (ODS) steels have been considered as candidates for fusion blanket structural materials [1] and cladding materials of next generation fission reactors [2–7]. They have high strength at elevated temperatures because of the ultra-fine oxide particles dispersion which contributes to strengthening of ODS steels with high thermal stability. During the hot extrusion process, the grains in the steel are elongated along with the extrusion direction, which causes the anisotropy in the ductility of the ODS steels [8]. Since tubing processing in the cladding fabrication enhances the anisotropy in ductility, the recrystallization is necessary to modify grain morphology for maintaining ductility of the tube in the radial direction. Thus, understanding recrystallization behavior is critical for ODS ferritic steels for practical application to cladding for nuclear fuels.

Annealing deformed metals at elevated temperatures results in an alteration of microstructures through the processes of recovery, recrystallization and grain growth. Here, we call this series of processes as recrystallization behavior, since the above processes often occur simultaneously and cannot be distinguished clearly. Since the recovery and recrystallization processes are accompanied

by dislocation motion and grain boundary migration, the oxide particles dispersed in the matrix are expected to influence the recrystallization behavior of ODS steels. Actually, recrystallization of ODS ferritic steels is harder than conventional ferritic steels because of the existence of oxide particles. However, it is considered that recrystallization temperature should be kept low enough to suppress too much growth of the grains and oxide particles, otherwise strength is lost [2]. Therefore adequate recrystallization treatment is essential for the practical application of ODS ferritic steels as cladding tubes. There are several factors determining recrystallization behavior, such as the conditions of cold rolling, annealing temperature/period and oxide particle dispersion morphology. Since the plastic strain may control internal strain energy that accelerates recrystallization [9,10], it is considered that the cold rolling process affects the following recrystallization behavior. Since the pinning effect on grain boundary migration by oxide particles is expected to be remarkably affected by the dispersion morphology of the particles, the recrystallization behavior can be different between Al-added and Al-free ODS steels where the dispersion morphology is different because of the difference of oxide particles dispersed in each steel [11,12].

In this research, the effects of cold rolling on recrystallization behavior are investigated for Al-free and Al-added 15Cr-ODS ferritic steels with different oxide particle morphology. Cold rolling with different reduction ratio is carried out in two directions according to the extrusion direction (ED); one is the case where the ED is parallel to the rolling direction (RD) and another is that the ED is parallel to the transverse direction (TD). The effect of a repeated process of cold rolling/recrystallization, which is called a double-recrystallization processing, is also investigated for both of the steels.

2. Materials and Methods

2.1. Materials

The ODS steels used in this study are an Al-added ODS ferritic steel, composed of Fe (Bal.)-14.5Cr-2W-3.3Al-0.51Zr and an Al-free ODS steel, Fe (Bal.)-13.6Cr-2W-0.16Ti. The chemical compositions are shown in Table 1. These ODS ferritic steels were fabricated by means of mechanical alloying method as shown in Figure 1. The pre-alloyed powders and Y₂O₃ powder were mechanically alloyed by an attriter under Ar gas atmosphere. The mechanical alloying was performed at a rotation speed of 220 rpm for 48 h. After mechanical alloying, fine powders were sieved out and encapsulated into a capsule made of a mild steel. After the capsules were degassed in a vacuum of 10⁻³ torr at 400 °C for 3 h, hot extrusion was carried out at 1150 °C to shape into a rod with 25 mm diameter. Through several experiences of material fabrication processing, relatively large oxide particles of Al-Y complex oxide are observed in Al-added ODS steel, and these particles are believed to cause poor mechanical properties. As for the effect of Zr on dispersion morphology of the oxide particles, the details will be shown elsewhere.

Table 1. Chemical compositions of the ODS steels. The composition of Y₂O₃* is that of measured Y₂O₃ powder, and Ex.O** is a substitution of O forming Y₂O₃ from the measured total O in the steels.

Fe(Bal.)	C	Si	Mn	P	S	Cr	W	Al	Ti	Y	O	N	Ar	Zr	Y ₂ O ₃ *	Ex. O**
15Cr-4Al-2W	0.03	0.02	0.02	<0.005	0.001	14.7	1.9	3.3	-	0.26	0.11	0.004	0.006	0.51	0.33	0.04
15Cr-2W	0.05	0.03	0.03	<0.005	0.001	13.6	1.9	0.02	0.16	0.26	0.11	0.004	0.006	-	0.33	0.04

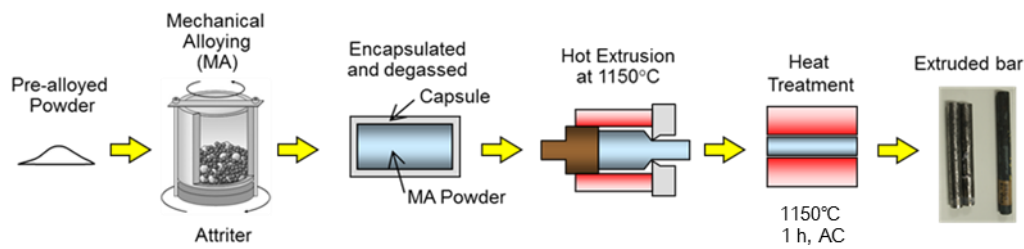


Figure 1. Processing of mechanical alloyed ODS ferritic steels for production of the extruded bar. Pre-alloyed powder with an addition of Y_2O_3 powder was mechanically alloyed in an attriter with steel balls for 48 h in Ar. Hot extrusion was performed at 1150 °C, and homogenization annealing was done at 1150 °C for 1 h followed by air cooling. The diameter of the extruded bar was about 25 mm.

2.2. Cold Rolling

2.2.1. Recrystallization Behavior

The bulk specimens with different thickness were sampled from the center of the extruded bar with the geometries of $10 \times 10 \times 1\text{--}3 \text{ mm}^3$. As-extruded materials were cold rolled in the extrusion direction, which is named as the RD direction (Figure 2a). The reduction ratio of specimen thickness was 20%, 40% and 80% for both Al-free and Al-added ODS steels, and each specimen was subjected to isothermal annealing in a vacuum at temperatures from 850 °C to 1400 °C with 50 °C steps for 1 h, as shown in Figure 3. Heating rate for the annealing was 30 °C/min and the specimens were cooled in the furnace. Vickers hardness tests and microstructure observations were carried out after each isothermal annealing. All annealing processes were performed by using a hot press machine.

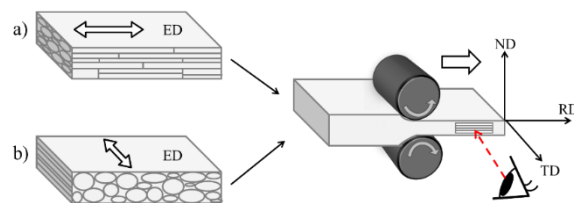


Figure 2. Schematic view of cold rolling direction and the extrusion direction (ED): (a) the ED is parallel to the RD, and (b) the ED is parallel to the transverse direction (TD). Most of the rolling directions are the case (a) in this study except for mentioning. ND is the normal direction of rolling surface.

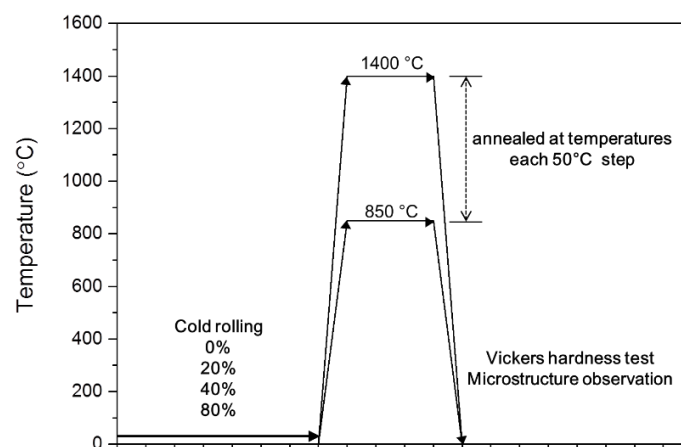


Figure 3. Isothermal annealing to investigate recrystallization behavior of cold rolled 15Cr-ODS ferritic steels with and without Al addition. As-received materials consolidated by hot extrusion processing were cold rolled with 20, 40, 80% reduction of area, and each cold rolled specimen was isothermally annealed for 1 h at each temperature from 850 °C to 1400 °C with 50 °C steps.

2.2.2. Effects of Prior Recrystallization and the Rolling Direction

As for the practical tube manufacturing, several cycles of a set of cold rolling-annealing processing were often conducted [13–16]. As shown in Figure 4, before the isothermal recrystallization annealing, a series of cold rolling and recrystallization annealing was performed prior to the isothermal annealing experiment. Here, we call this a double-recrystallization processing. The pre-treatment was such that for as-received materials being 40% cold rolled and annealed at just below the recrystallization temperature, which is 900 °C for Al-added and 1200 °C for Al-free ODS steels. Then, the second cold rolling with a 40% reduction ratio was performed, and followed by the isothermal annealing for 1 h at temperatures between 850 °C and 1400 °C with steps of 50 °C.

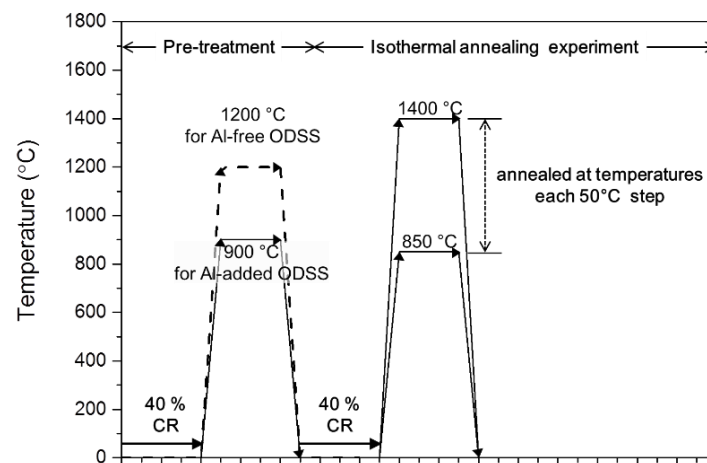


Figure 4. A series of cold rolling and recrystallization annealing was performed prior to the isothermal annealing experiment. The pre-treatment was such that for as-received materials being 40% cold rolled and annealed at just below the recrystallization temperature which is 900 °C for Al-added and 1200 °C for Al-free ODS steels. Then, the second cold rolling with 40% reduction ratio was performed and followed by the isothermal annealing for 1 h at temperatures between 850 °C and 1400 °C with steps of 50 °C. The isothermal annealing with and without pre-treatment are called dual and single processing. Here, the rolling direction of first and second rolling was parallel to the extruded direction.

In order to investigate the effects of cold rolling direction, another cold rolling was performed in the direction perpendicular to the extrusion direction, which is called the TD, only for those with a 40% reduction ratio (Figure 2b).

2.3. Materials Characterizations

Hardness measurements were performed after the isothermal annealing. The surface of the specimen was mechanically grinded with emery SiC papers until #4000, and buff-polished with a diamond paste of 6 µm diameter. Micro-Vickers hardness tests for each cold rolled specimen before and after isothermal annealing were carried out with a load of 1 kgf for 10 s. Ten data were averaged as the hardness with excluding the maximum and minimum values of the twelve measurements. The errors of Vickers hardness are mostly within ± 12 Hv.

For the microstructure observations, the annealed samples were mechanically ground and buff-polished with diamond paste of 6, 3, 1, 0.25 µm diameter. Finally, colloidal silica polishing with 0.04 µm diameter was performed. The grain morphology was observed by a scanning electron microscope (SEM) installed in field emission type electron probe micro analyzer (FE-EPMA), JXA-8500FK (JEOL co, Tokyo, Japan). Electron backscatter diffraction (EBSD) analysis was carried out to obtain crystallographic information. The specimens for transmission electron microscope (TEM) observation were sampled from the plates with each cold rolling ratio after recrystallization treatment of Al-added and Al-free ODS steels by focused ion beam (FIB) technique using JFIB-2100 (JEOL co,

Tokyo, Japan) and FB-2200 (Hitachi High technologies co, Tokyo, Japan). Thin foil samples, which measure $5 \times 10 \times 0.1 \mu\text{m}^3$, were prepared by Ga-ion bombardment and put on a Cu mesh. The surface damage layer induced by ion bombardment was removed by a gentle milling apparatus [17]. The effect of annealing on the oxide particle distribution morphology was examined by TEM (JEM-2010, JEOL co., Tokyo, Japan) with an acceleration voltage of 200 kV. All the TEM micrographs were observed from the TD direction as shown in Figure 2.

3. Results and Discussion

3.1. Annealing Effect on Extruded Al-Free and Al-Added ODS Ferritic Steels

3.1.1. Hardness Change

Figure 5 shows the effect of cold rolling ratio on Vickers hardness changes by isothermal annealing in both Al-added and Al-free ODS ferritic steels consolidated by hot extrusion method, where the Vickers hardness is reduced as increasing annealing temperature as expected. The hardness of Al-free ODS steel is always higher than that of Al-added ODS steel, except for the 80% cold rolled specimen after annealing to temperatures above 1300 °C. Before annealing, hardness is highest in the 80% cold rolled specimen, which is due to cold work by generation of dislocations in the highest density. The hardness is abruptly decreased with increasing annealing temperature. In general, the temperature showing an abrupt hardness reduction decreases while increasing the reduction ratio of cold rolling. It is considered that the abrupt reduction of hardness is due to annealing out of point defects and dislocations generated by the cold rolling, which is well known as recovery of cold work.

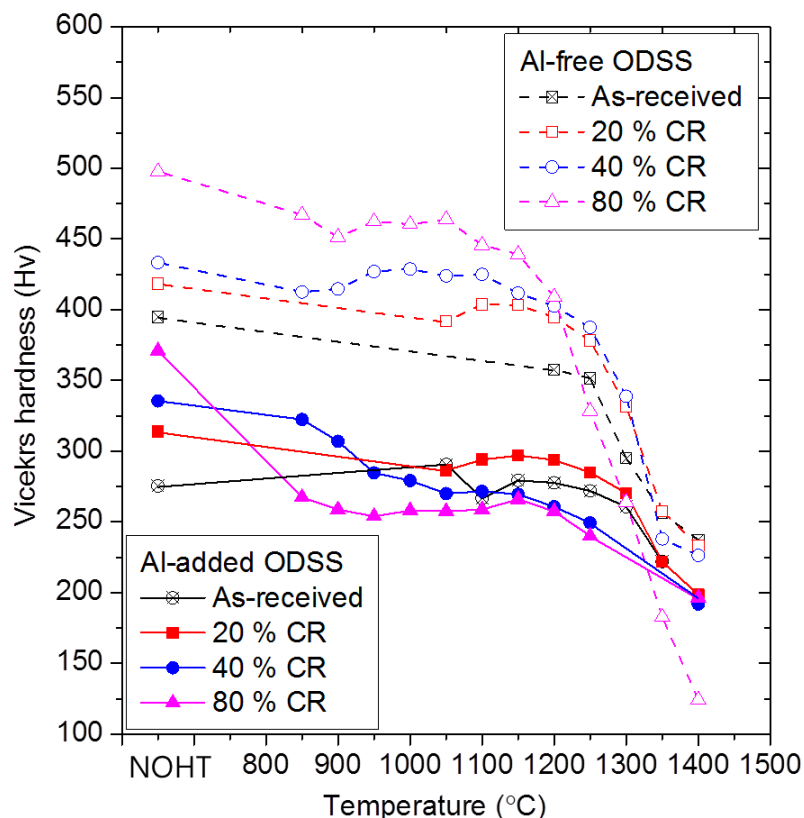


Figure 5. Vickers hardness changes of Al-added and Al-free 15Cr-ODS ferritic steels consolidated by extrusion method after isothermal annealing for 1 h at temperatures from 850 °C to 1400 °C with 50 °C steps. Before the annealing, specimens were cold rolled (CR) with 20%, 40% and 80% reduction of area. NOTH stands for no heat treatment.

In the case of Al-added ODS steel, the hardness of a 20% cold rolled specimen is considerably reduced at around 1350 °C, which is similar to the as-received specimen. The annealing temperature showing a considerable reduction of hardness is around 950 °C in the 40% cold rolled specimen and 850 °C in the 80% cold rolled specimen. In Al-added ODS steel, a similar trend with Al-free ODS steel was observed: The hardness reduction starts at a lower annealing temperature for the specimens with higher reduction ratio. The hardness of the 40% and 80% cold rolled specimen are significantly decreased at around 1300 °C and 1250 °C, respectively.

It is noted that in the annealing temperature range between 850 °C and 1250 °C, the difference in hardness among the cold rolled specimens is much larger in Al-free ODS steels. This clearly indicates that the dislocations generated by cold rolling are much more stable in the Al-free ODS steel compared to those in the Al-added ODS steel, which is probably due to the pinning of dislocations by finely-dispersed oxide particles in Al-free ODS steel [18], indicating a significant retardation of recovery. In the practical tubing processing, as workability is one of the key issues to prevent from shearing fracture of the tube, an appropriate cold rolling ratio should be chosen for processing tubing from Al-free ODS ferritic steels with consideration of recovery of dislocations.

3.1.2. Grain Morphology Change

Figure 6 shows the examples of grain morphology change by annealing at different temperatures for both the ODS steels with different cold rolling ratio. These grain morphologies show characteristic features after annealing at each temperature where the Vickers hardness decreased depending on the annealing temperature, the cold rolling ratio and the Al content of the ODS steel.

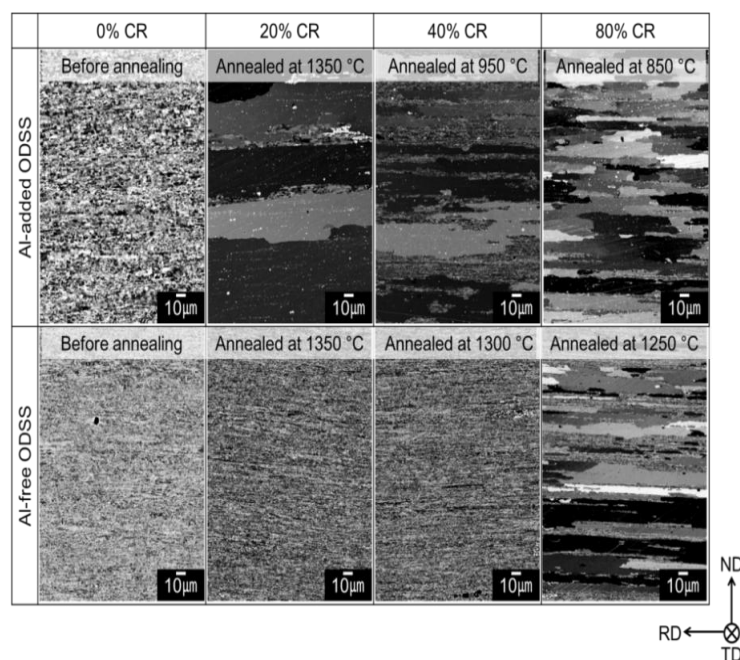


Figure 6. Grain morphology of Al-added and Al-free 15Cr-ODS ferritic steels after annealing at each temperature. In both the steels after annealing, the hardness is not changed among the specimens shown here. Cold rolling was performed before isothermal annealing.

The grain morphology was changed by annealing much more significantly in Al-added ODS steel than that of Al-free. The microstructure observation revealed that recrystallization occurred in all the specimens shown in the figure. The grain size of the 20% cold rolled specimen of Al-added ODS steel is significantly increased after annealing at 1350 °C, and the 40% cold rolled specimen has smaller grains than that of the 20% cold rolled one, due to a lower annealing temperature of 950 °C.

The Al-added steel with 80% cold rolling shows the smallest recrystallized grains after annealing at 850 °C, of which the Vickers hardness is abruptly reduced by the annealing. It is considered that the reduction of the hardness is due to not only recrystallization, but also the other microstructures such as oxide particle dispersion morphology. Grain growth is accompanied by an abrupt reduction of hardness, which becomes more significant in the specimen with a small cold rolling ratio. This is due to a higher annealing temperature than in the specimen with a small cold rolling ratio. It can be said that the factors controlling hardness of the ODS steels after recrystallization are not only the grain size, but oxide particle dispersion morphology, which significantly depend on the annealing temperature.

The recrystallization behavior of Al-free ODS steel is considerably different from that of Al-added ODS steel. The 20% cold rolled Al-free ODS steel never shows recrystallization or grain growth, even after the annealing at 1350 °C. The 80% cold rolled specimen of Al-free ODS steel recrystallized at above 1250 °C. It is again confirmed that Al-free ODS steel is still hardly recrystallized after cold rolling processing. As mentioned in Section 3.1.1., finely dispersed oxide particles in Al-free ODS steel effectively retard recrystallization by pinning grain boundaries as well as dislocations.

At moderate high temperatures below 850 °C, the recovery occurs by rearranging point defects and dislocations into low-angle grain boundaries. The driving force is the difference in internal energy between the deformed and recrystallized state, ΔE per unit volume, which can be correlated with the dislocation density or the sub-grain size and surface energy as shown by Equation (1) [18]:

$$\Delta E \approx \rho G b^2 \approx 3 \gamma_s / d_s \quad (1)$$

where ρ is the dislocation density, G is the shear modulus, b is the Burgers vector of the dislocations. γ_s is the sub-grain boundary energy and d_s is the sub-grain diameter. Because the internal stress is too small to recrystallize at a low cold rolling ratio, the annealing at a higher temperature up to 1350 °C is required for recrystallization in the strongly textured ODS ferritic steels. With increasing cold rolling ratio, the stored energy is increased, and recovery is accelerated. The 80% cold rolling makes recrystallization start at a lower temperature.

As shown in Figure 5, the annealing above 850 °C in Al-free ODS steel caused an increase in the hardness before an abrupt decrease in hardness. It is expected that in this annealing temperature range recrystallization as well as recovery occurs, and a small amount of grain boundary modification may change the dislocation barrier strength to cause hardening. In Al-added ODS steel, however, this phenomenon was not observed, with no remarkable increase in the annealing curves of the hardness of each specimen with different cold rolling ratio. As mentioned before, the hardness of the Al-added ODS steel specimens annealed at different conditions shown in Figure 6, is almost the same among three annealed specimens, although the grain morphology is significantly different from each other. This clearly indicates that the hardness of the ODS steels after recrystallization was not controlled by grain size only, but by the other factors like oxide particle dispersion morphology and dislocation density, of which the significance is larger in Al-added ODS steel than Al-free ODS steel.

3.1.3. Deformation Texture

Deformation texture was examined by EBSD analysis, and pole figures are shown in Figure 7, before and after annealing at each temperature, which is same as shown in Figure 6. Before annealing, all the pole figures indicate that the $\langle 110 \rangle$ deformation texture developed along with the extrusion direction denoted as RD. The grain orientations are allocated on the edge of the stereo triangle connecting $\langle 001 \rangle$ and $\langle 111 \rangle$, which enables the definition of the texture as $\{112\} \langle 110 \rangle$ orientation. The grains are elongated in parallel to the extrusion direction (ED), which is the cold rolling direction in this case. By increasing the cold rolling reduction ratio, the more dense RD fiber is formed in both the ODS steels.

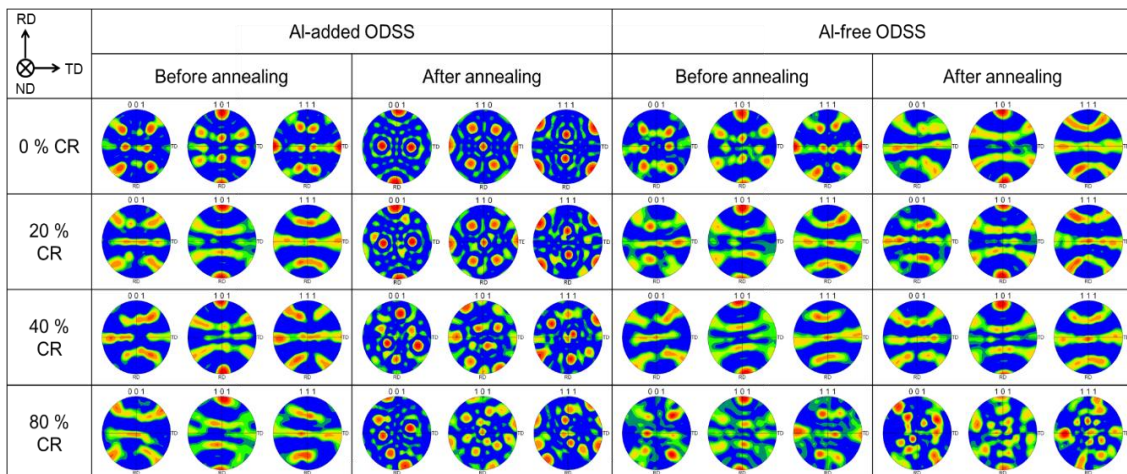


Figure 7. Pole figures of EBSD deformation texture before and after annealing at each temperature, are the same as the conditions shown in Figure 6. Grain morphology of Al-added and free 15Cr-ODS ferritic steels after annealing at each temperature. Cold rolling was performed before isothermal annealing.

After annealing, the pole figure changes in accordance with the annealing temperature and cold rolling ratio. The pole figure of the 20% cold rolled Al-added ODS steel after the annealing at 1350 °C indicates almost no texture in the extrusion direction, which agrees with the well-grown grains in Figure 6. The orientation is $\{110\} \langle 100 \rangle$, indicating a sharp Goss orientation in secondary recrystallization, which is same with that after recrystallization without cold rolling. In the 80% cold rolled Al-added ODS steel, it is also shown that recrystallization relieves the strong deformation texture along with the extrusion direction. Furthermore, the grain orientations appear to change from $\{112\}$ to $\{110\}$, of which the trend agrees well with the progress in the secondary recrystallization, and $\{112\}$ and $\{113\}$ texture is strong in the 80% cold rolled Al-added ODS steel. These behaviors appear to not be changed by the presence of oxide particles.

The Al-free ODS steel with 20% and 40% cold rolling shows no change in the pole figure after the annealing, while 80% cold rolled specimen shows a change in the pole figure showing rather random deformation structure. This trend reflects the change in the grain morphology from very fine grains to coarsened and elongated grains as shown in Figure 6. Therefore it is expected that the small hardening in the temperature range between 850 °C and 1200 °C is not due to the change in grain texture, but the change in grain boundary structure caused by a small grain boundary migration.

As for the effect of Al addition on the recrystallization behavior of the ODS steel, all the experimental results indicate that the recrystallization of 15Cr-ODS ferritic steel is enhanced by the addition of Al, which causes the reduction of strength. The hardness before annealing was affected by the addition of Al as shown in Figure 5, indicating that the hardness of Al-added and Al-free ODS steels are 275 MPa and 390 MPa, respectively. Since the grain sizes of both the steels are almost same, this difference in the hardness is considered to be due to the difference in the oxide particles dispersion morphology, which is discussed in the next session.

3.1.4. Observation of Dispersed Oxides

Recrystallization is accompanied by grain nucleation and growth through a large amount of grain boundary migration. In the ODS steels, dispersed oxide particles play a role to pin down the grain boundary migration to cause retardation of recrystallization. Figure 8 shows the dispersion morphology of oxide particles at each condition for extruded Al-free and Al-added 15Cr-ODS steels. Although the oxide particles in the as-received condition are fine, those after the annealing are significantly coarser than in the as-received condition. For example, the averaged diameter of the oxides in Al-added ODS steel was estimated to be larger than 30 nm, as in the case of 1350 °C after 20%-CR. As for Al-free ODS steel, the microstructure was surprisingly stable, showing almost no significant

change in grain morphology. In the previous study [2], it is suggested that Al-free ODS steels can obtain high strength at elevated temperatures because of their ultra-fine oxide particles such as Y-Ti-O complex. Consequently, it is suggested that the fine Y-Ti-O oxide particles restrain recrystallization by pinning grain boundaries in Al-free ODS steel, while Al-added ODS steel was easily recrystallized because of weak pinning by a low number density of large Y-Al-O oxide particles [11,12,17]. As for the 80% cold rolled Al-added ODS steel, the oxide particles annealed at 850 °C are not coarse, but similar size with those of as-received condition, because the annealing temperature is not as high as 1250 °C. It is noted that although recrystallization occurred at 1250 °C in Al-free 80%-CR ODS steel, oxide particles are smaller than those after annealing at 1300 °C of Al-free 40%-CR ODS steel.

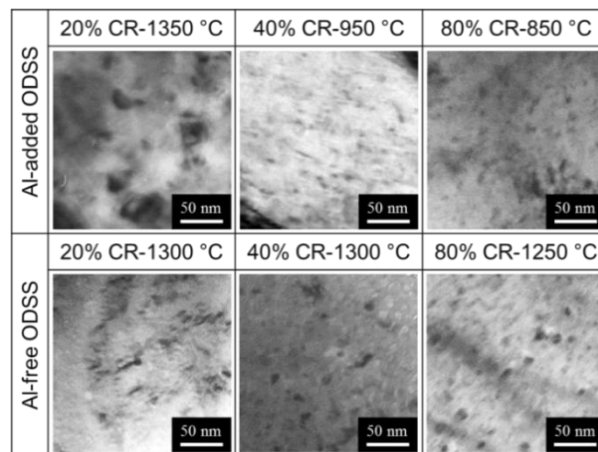


Figure 8. Dispersion morphology of oxide particles at each isothermal annealing condition for 15Cr-ODS ferritic steels with and without Al addition.

Oxide particle growth mostly depends on annealing temperature, while recrystallization and grain growth are controlled by multiple factors such as dislocation density, initial grain size and oxide particle dispersion morphology. Stored energy by cold rolling accelerates recovery and recrystallization in Al-free ODS steel. Therefore, it is suggested that recrystallization is easier with bigger oxide particles in matrix, as reported by Baker and Martin [19].

3.2. Effect of Cold Rolling Direction on Grain Morphology

As it is well known that body centered cubic (BCC) structured materials have preferred crystallographic orientations of texture induced by cold rolling, which are α -fiber and γ -fiber [20–23]. Because the cold rolling direction is the same as the extruded direction during the fabrication processing, the anisotropy remains in elongated grains after cold rolling [8]. Therefore, it is considered that the anisotropy might be affected by the cold rolling processing with the different cold rolling direction such as parallel or perpendicular to the extruded direction, which may be another factor controlling the grain shape in the plate manufacturing of ODS ferritic steels. Thus, the effect of the cold rolling direction on grain morphology and texture is investigated in this session.

Figure 9 is the effect of cold rolling on the 3D microstructure of deformation texture of Al-added ODS steel with a stereo-triangle of crystallographic orientation: a) as-extruded, b) 40%-CR and cold rolling direction is parallel to the extruded condition (ED), c) 40%-CR and cold rolling direction is perpendicular to the extruded condition (TD). Noted that each surface of 3D microstructure is not in conjunction with the single standard orientation of the rolling specimen surface, but they are just the orientation maps of observed surfaces. As shown in the texture of as-extruded condition a), the specimen already has elongated grains along with the extrusion direction. The top and front surface are similar to each other, but the side surface shows that many grains oriented in the $\langle 110 \rangle$ direction are as well-known as an α -fiber texture, that is, RD becomes parallel to $\langle 110 \rangle$ direction shown

with light green of stereo triangle. Figure 9b is of 40% cold rolling along with the rolling direction, which indicates that the orientation relationship is similar to that of as-extruded condition (Figure 9a), although the front surface indicates that cold rolling makes the grains be fine.

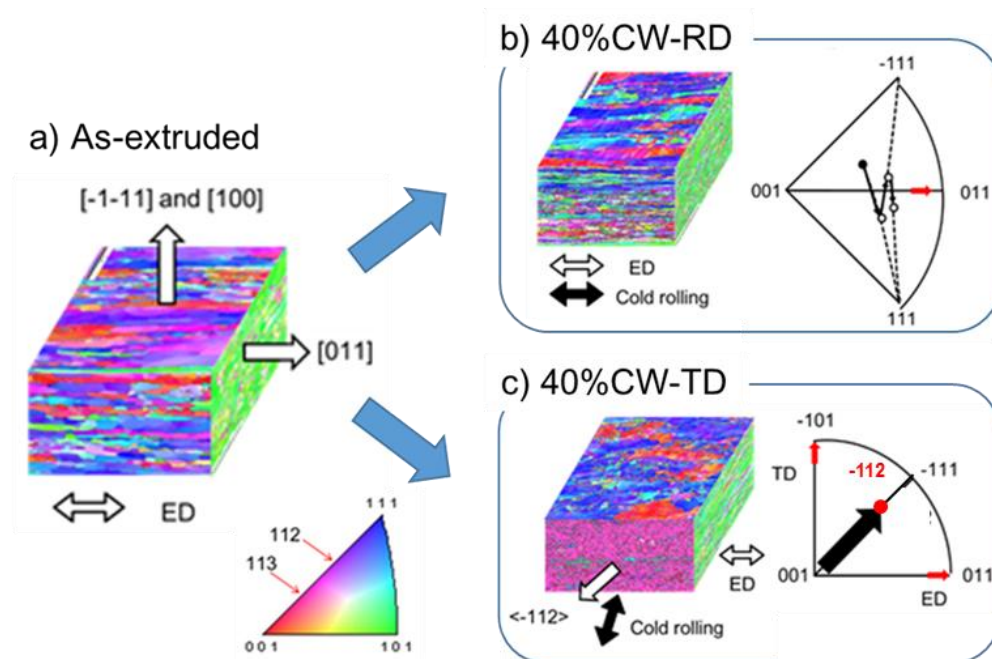


Figure 9. The effect of cold rolling on the 3D microstructure of deformation texture of Al-added ODS steel with a stereo-triangle of crystallographic orientation: (a) as-extruded, (b) 40%-CR and cold rolling direction is parallel to the extruded condition (ED), (c) 40%-CR and cold rolling direction is perpendicular to the extruded condition (TD). Noted that each surface of 3D microstructure is not conjunct with the single standard orientation of the rolling specimen surface, but they are just the orientation maps of observed surfaces.

In contrast to this, the cold rolling in the direction of the TD (Figure 9c) results in a different behavior, which is observed in the front surface, indicating that the orientation is now mainly rotated to $\{112\}$. The grain morphology has pushed away from the extruded direction, which may reduce the anisotropy, so it appears more equiaxed than that of RD specimen in high magnification. However, they still have an anisotropy along with extrusion direction.

Based on the results obtained by EBSD analysis as shown in Figure 9, the following texture formation mechanism is considered for the case of 40%-CR-RD. In BCC crystal, the slip direction is $\langle 111 \rangle$, and the specimen axis rotates to $[111]$ first. Once the axis overshoots the triangle line of $[001]$ – $[011]$ edge, the axis rotation is now conversed to the $[-111]$ orientation. This double slip deformation leads to the final rotation of slip direction to the $[011]$ orientation, which causes the formation of α -fiber texture in the extruded ODS steel. In contrast, after the cold rolling perpendicular to the extruded direction (TD), the grain orientation changes as shown Figure 9c. In this case, similar rotation occurs, but the rotation direction is not the $[011]$, but the $[-101]$, which is marked by the red arrow with the TD. It is considered that the rotation can be proceeding to the combination of two rotations (one is extruded direction and another one is cold rolling direction), and the combined direction of the axis can be $[-112]$. This indicates that the axis rotates along the edge of the triangle $[001]$ / $[-111]$, as marked black arrow. There is the $[-112]$ on this edge indicated in Figure 9c.

In order to investigate the recrystallization behavior after mixed cold rolling direction in Al-free ODS steel, the TD cold rolled specimen was annealed at 1000°C for 1 h. Figure 10 is the structure of (a) as-extruded, (b) extruded and 40% cold rolled in the TD and (c) extruded, 40% cold rolled and annealed at 1000°C for 1 h, indicating that the grain morphology and orientation of these three cases

are not significantly changed compared with Al-added ODS steel. This is considered to be due to suppression effect by much stronger pinning effects on grain boundaries by Y-Ti-O oxide particles formed in Al-free ODS steel. A part of grains shows grain growth of which the crystal orientation of normal direction (ND) is $\langle 111 \rangle$ that is consistent to the previous results on BCC iron [24].

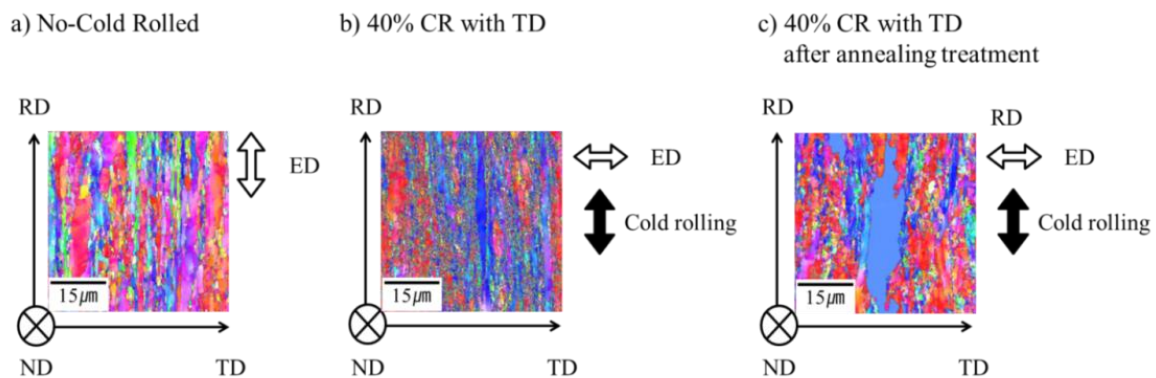


Figure 10. Grain morphology on ND surface in Al-free ODS steel; (a) as-extruded, (b) extruded and 40% cold rolled in the TD and (c) extruded, 40% cold rolled and annealed at 1000 °C for 1 h.

3.3. Grain Morphology of Double-Recrystallization Processed ODS Steels

During the fabrication processing, cladding tubes were subjected by several cycles of annealing and cold rolling to reduce the wall thickness, while keeping enough ductility of ODS steel for tubing. Figure 11 shows the effect of prior treatment of 40%-CR + recrystallization annealing on the Vickers hardness changes by isothermal annealing for 1 h at each temperature from 850 °C to 1400 °C with 50 °C step for both the Al-free and Al-added 15Cr-ODS steels (see Figure 3), where the prior annealing temperature was selected to be 900 °C in Al-added ODS steel and 1200 °C in Al-free ODS steel. Both the steels were isothermally annealed with and without pre-treatment, as indicated in Figure 3 where the isothermal annealing with and without pre-treatment were called double and single processing. Here, the rolling direction of first and second rolling was parallel to the extruded direction.

It can be said that the isothermal annealing behavior of both the steels are not remarkably affected by the presence of the pre-treatment of 40%-CR + recrystallization treatment. However, the hardness of Al-free ODS steel after double processing was suddenly reduced at around 1350 °C, and finally reached to the lowest hardness of about 150 Hv, while no change was observed up to 1250 °C. In the case of Al-added ODS steel, the hardness change occurred gradually, and no effect of pre-treatment was observed. The similar annealing temperature dependence in the hardness of both steels indicates that the prior treatment gives no effect on the second annealing behavior, since the grain morphology of both steels are not changed remarkably by the prior annealing.

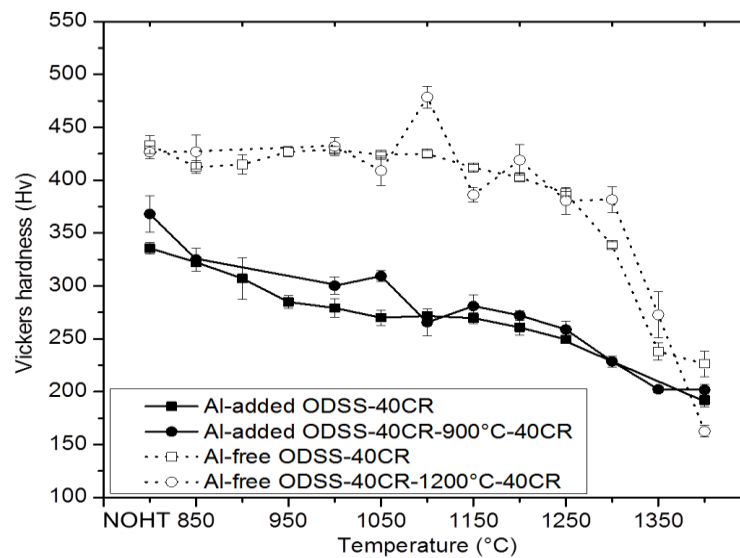


Figure 11. The effect of prior treatment of 40%CR + recrystallization annealing on the Vickers hardness changes by isothermal annealing for 1 h at each temperature from 850 °C to 1400 °C, with 50 °C step for both the 15Cr-ODS steels with and without Al addition (see Figure 3), where the prior annealing temperature was selected to be 900 °C in Al-added ODS steel and 1200 °C in Al-free ODS steel. NOTH stands for no heat treatment.

Figure 12 shows the change in grain morphology after double processing in both the steels. In Al-added ODS steel, the fine microstructures were partially recrystallized at 1000 °C, indicating that the recrystallization partially started at this temperature. After annealing at 1300–1350 °C, the grains are almost fully recrystallized. Al-free ODS steel, however, is more difficult to recrystallize than Al-added ODS steel, and in the case of the dual processing, recrystallization started at around 1300 °C, which is about 300 °C higher than Al-free ODS steel. Therefore, the dislocation pinning by fine oxide particles is not affected by cyclic cold rolling/recrystallization treatment.

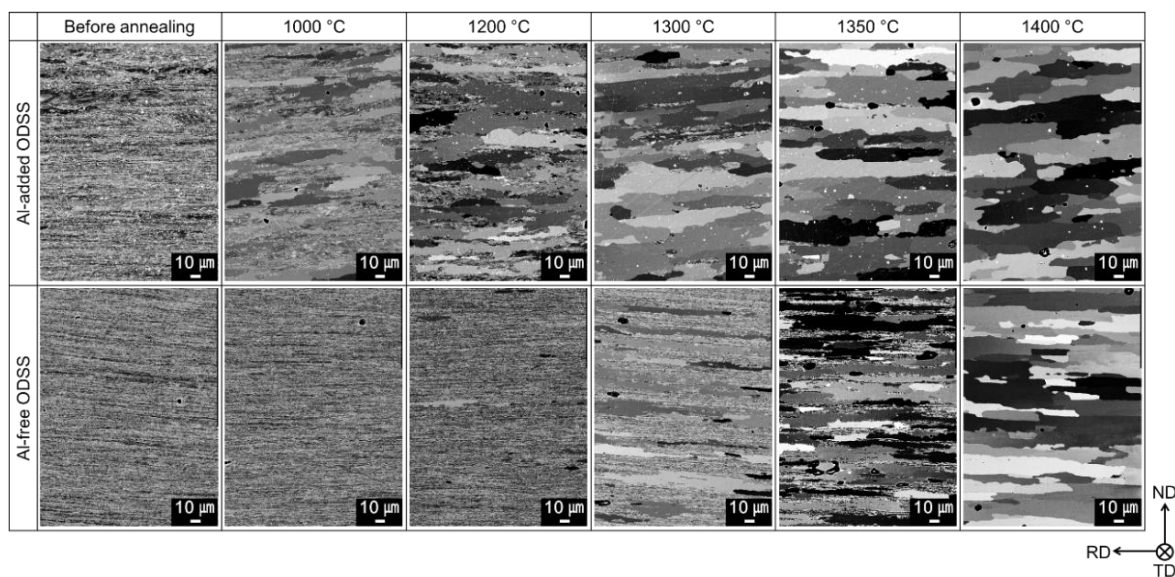


Figure 12. The change in grain morphology after dual processing in 15Cr-ODS ferritic steels with and without cold rolling.

In the practical tubing processing of ODS ferritic steels, the selection of annealing temperature for recrystallization, or even recovery is critical. The most important is that tubing requires ductility as well as strength, otherwise the tube may break by cracking or shearing. For maintaining the strength of ODS steels, finely dispersed oxide dispersion is demanded, whereas for keeping the ductility of the steels, anisotropy should be reduced. Since the reduction of anisotropy can be achieved by recrystallization, in general, the ODS ferritic steels were annealed at temperatures higher than so-called recrystallization temperature. However, since the high temperature recrystallization often results in coarsening of the oxide particles, the temperature should be set at as low as possible. This dilemma of the selection recrystallization temperature makes tubing processing being not easy.

For tube processing of ODS ferritic steel from a rod of 20 mm diameter to 10 mm outer diameter of cladding, four sets of tubing/annealing were performed in our previous works [2–8]. Although the number of cycles of this treatment depends on the starting material shape, the reduction rate of tube wall thickness should not be too large, and several cycles of tubing/annealing process are required. Because it is clear that the hardness reduction by annealing is affected by the grain morphology, in the practical tubing process, the appropriate annealing (recrystallization) temperature could be chosen on the bases of the annealing behavior of hardness depending on temperature, annealing period and cold work ratio as suggested earlier.

Figure 13 shows the results of EBSD analysis before and after annealing at 1400 °C of both Al-added and Al-free ODS steel. Before annealing, both the ODS steels have grains with $\{111\}/\{100\} <110>$ orientation in the TD direction, which corresponds to α -fibre texture. Al-added ODS steel has many sub-grains in the large grains as indicated with white lines of misorientation angle below 5 degree. After annealing at 1400 °C, both the ODS steels are recrystallized and grain growth occurs.

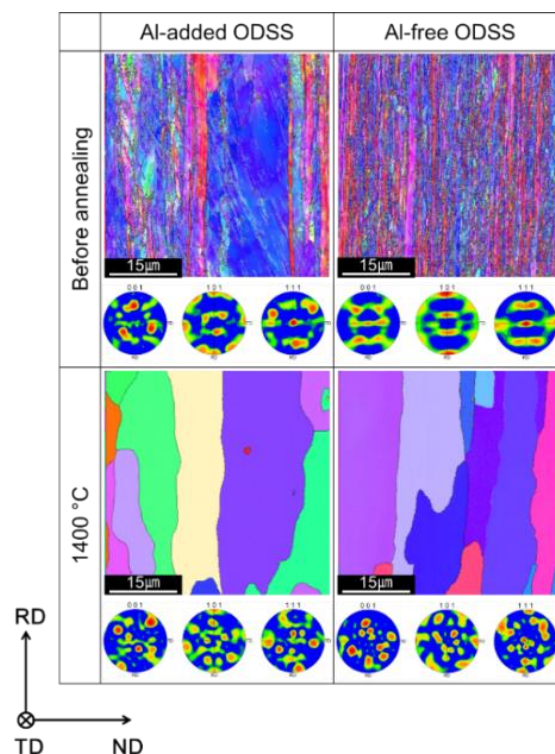


Figure 13. Grain orientation map and pole figure of EBSD analysis before and after annealing at 1400 °C of both Al-added and Al-free ODS ferritic steel.

Finally, it is estimated that the recrystallization temperature of Al-free and Al-added 15Cr-ODS ferritic steel is 900 °C and 1250 °C with the annealing period of 1 h.

4. Conclusions

The effect of cold rolling on recrystallization behavior of 15Cr-ODS ferritic steels with and without addition of Al was investigated. The change in microstructure is particularly noticeable for different cold rolling and annealing conditions. The results obtained are summarized as follows;

- The recrystallization of both steels are enhanced by cold rolling. The Al-free ODS steel with finer oxide particles is harder to recrystallize than Al-added ODS steel with coarser oxide particles.
- The effect of Al addition on the recrystallization behavior is evident. It is estimated that the recrystallization temperature of Al-free and Al-added 15Cr-ODS ferritic steel is 900 °C and 1250 °C with the annealing period of 1 h.
- In Al-free ODS steel a small hardening was observed in the temperature range between 850 °C and 1200 °C, while no such phenomenon was observed in Al-added ODS steel, which is indicative of retardation of recovery by finely dispersed oxide particles.
- Oxide particle growth is mostly depending on annealing temperature, while recrystallization and grain growth are controlled not only by the temperature, but also by the cold rolling ratio, which alter the multiple factors such as dislocation density, initial grain shape and oxide particle dispersion morphology.
- The cold rolling direction also influences the grain morphology and grain orientation in Al-added ODS steel, and the second rolling to the perpendicular direction to the first cold rolling direction induces the rotation of the grains from $\langle 110 \rangle$ to $\langle 112 \rangle$.
- The recrystallization temperature is not significantly changed by cold rolling direction. Recrystallization after cold rolling appears to increase the $\{111\}$ grain orientation on the cold rolled specimen surface.

Author Contributions: Conceptualization, Y.H. and A.K.; methodology, Y.H.; validation, Y.H.; formal analysis, Y.H.; investigation, Y.H.; resources, X.X.; data curation, X.X.; writing—original draft preparation, Y.H.; writing—review and editing, A.K.; visualization, Y.H.; supervision, A.K.; project administration, A.K.; funding acquisition, A.K.

Funding: This research received no external funding.

Conflicts of Interest: The authors declare no conflict of interest.

References

1. Zinkle, S.J.; Snead, L.L. Designing Radiation Resistance in Materials for Fusion Energy. *Annu. Rev. Mater. Res.* **2014**, *44*, 241–267. [[CrossRef](#)]
2. Kimura, A.; Kasada, R.; Iwata, N.; Kishimoto, H.; Zhang, C.H.; Isselin, J.; Dou, P.; Lee, J.H.; Muthukumar, N.; Okuda, T.; et al. Development of Al added high-Cr ODS steels for fuel cladding of next generation nuclear systems. *J. Nucl. Mater.* **2011**, *417*, 176–179. [[CrossRef](#)]
3. Cho, H.S.; Kimura, A.; Ukai, S.; Fujiwara, M. Corrosion Properties of Oxide Dispersion Strengthened Steels in Super-Critical Water Environment. *J. Nucl. Mater.* **2004**, 329–333, 387–391. [[CrossRef](#)]
4. Cho, H.S.; Ohkubo, H.; Iwata, N.; Kimura, A.; Ukai, S.; Fujiwara, M. Improvement of compatibility of advanced ferritic steels with super critical pressurized water toward a higher thermally efficient water-cooled blanket system. *Fusion Eng. Des.* **2006**, *81*, 1071–1076. [[CrossRef](#)]
5. Takaya, S.; Furukawa, T.; Aoto, K.; Müller, G.; Weisenburger, A.; Heinzl, A.; Inoue, M.; Okuda, T.; Abe, F.; Ohnuki, S.; et al. Corrosion behavior of Al-alloying high Cr-ODS steels in lead-bismuth eutectic. *J. Nucl. Mater.* **2009**, 386–388, 507–510. [[CrossRef](#)]
6. Isselin, J.; Kasada, R.; Kimura, A. Corrosion behaviour of 16%Cr-4%Al and 16%Cr ODS ferritic steels under different metallurgical conditions in a supercritical water environment. *Corros. Sci.* **2010**, *52*, 3266–3270. [[CrossRef](#)]
7. Isselin, J.; Kasada, R.; Kimura, A. Effects of Aluminum on the Corrosion Behavior of 16%Cr ODS Ferritic Steels in a Nitric Acid Solution. *J. Nucl. Sci. Technol.* **2011**, *48*, 169–171. [[CrossRef](#)]

8. Kasada, R.; Lee, S.G.; Isselin, J.; Lee, J.H.; Omura, T.; Kimura, A.; Okuda, T.; Inoue, M.; Ukai, S.; Ohnuki, S.; et al. Anisotropy in tensile and ductile–brittle transition behavior of ODS ferritic steels. *J. Nucl. Mater.* **2011**, *417*, 180–184. [[CrossRef](#)]
9. Leng, B.; Ukai, S.; Sugino, Y.; Tang, Q.; Narita, T.; Hayashi, S.; Wan, F.; Ohtsuka, S.; Kaito, T. Recrystallization Texture of Cold-rolled Oxide Dispersion Strengthened Ferritic Steel. *ISIJ Int.* **2011**, *51*, 951–957. [[CrossRef](#)]
10. Hölscher, M.; Raabe, D.; Lücke, K. Rolling and recrystallization textures of bcc steels. *Steel Res.* **1991**, *62*, 567–575. [[CrossRef](#)]
11. Dou, P.; Kimura, A.; Okuda, T.; Inoue, M.; Ukai, S.; Ohnuki, S.; Fujisawa, T.; Abe, F. Polymorphic and coherency transition of Y–Al complex oxide particles with extrusion temperature in an Al-alloyed high-Cr oxide dispersion strengthened ferritic steel. *Acta Mater.* **2011**, *59*, 992–1002. [[CrossRef](#)]
12. Dou, P.; Kimura, A.; Kasada, R.; Okuda, T.; Inoue, M.; Ukai, S.; Ohnuki, S.; Fujisawa, T.; Abe, F. TEM and HRTEM study of oxide particles in an Al-alloyed high-Cr oxide dispersion strengthened steel with Zr addition. *J. Nucl. Mater.* **2014**, *444*, 441–453. [[CrossRef](#)]
13. Ukai, S.; Nishida, T.; Okuda, T.; Yoshitake, T. Development of Oxide Dispersion Strengthened Steels for FBR Core Application, (II). *J. Nucl. Sci. Techn.* **1998**, *35*, 294–300. [[CrossRef](#)]
14. Mehtonen, S.V.; Karjalainen, L.P.; Porter, D.A. Hot deformation behavior and microstructure evolution of a stabilized high-Cr ferritic stainless steel. *Mater. Sci. Eng. A* **2013**, *571*, 1–12. [[CrossRef](#)]
15. Sornin, D.; Grosdidier, T.; Malaplate, J.; Tiba, I.; Bonnaillie, P.; Allain-Bonasso, N.; Nunes, D. Microstructural study of an ODS stainless steel obtained by Hot Uni-axial Pressing. *J. Nucl. Mater.* **2013**, *439*, 19–24. [[CrossRef](#)]
16. Unifantowicz, P.; Oksiuta, Z.; Olier, P.; de Carlan, Y.; Baluc, N. Microstructure and mechanical properties of an ODS RAF steel fabricated by hot extrusion or hot isostatic pressing. *Fusion Eng. Des.* **2011**, *86*, 2413–2416. [[CrossRef](#)]
17. Abe, M.; Kokabu, Y.; Hayashi, Y.; Hayami, S. Effect of grain boundaries on the cold rolling and annealing textures of pure iron. *Trans. Jpn. Inst. Met.* **1982**, *23*, 718–725. [[CrossRef](#)]
18. Dou, P.; Kimura, A.; Kasada, R.; Okuda, T.; Inoue, M.; Ukai, S.; Ohnuki, S.; Fujisawa, T.; Abe, F. Effects of Titanium Concentration and Tungsten Addition on the Nano-Mesoscopic Structure of High-Cr Oxide Dispersion Strengthened (ODS) Ferritic Steels. *J. Nucl. Mater.* **2013**, *442*, 95–100. [[CrossRef](#)]
19. Baker, I.; Martin, J.W. Effect of fine second phase particles on deformation structure in cold rolled copper single crystals. *Mater. Sci. Technol.* **1983**, *17*, 459–468. [[CrossRef](#)]
20. Leffers, T. On the misfit between the grains in a deformed sachs polycrystal and its relation to the inhomogeneous deformation of real polycrystals. *Scr. Met.* **1975**, *9*, 261–264. [[CrossRef](#)]
21. Smallman, R.E.; Lee, C.S. Advances in the theory of deformation and recrystallization texture formation. *Mater. Sci. Eng. A* **1994**, *184*, 97–112. [[CrossRef](#)]
22. Patra, S.; Ghosh, A.; Sood, J.; Singhal, L.K.; Podder, A.S.; Chakrabarti, D. Effect of coarse grain band on the ridging severity of 409L ferritic stainless steel. *Mater. Des.* **2016**, *106*, 336–348. [[CrossRef](#)]
23. Tsuji, N.; Hyoue, T.; Tsuzaki, K.; Maki, T. Effect of constraint on the rolled microstructure of (001)[100] oriented single crystals in an Fe-19%Cr ferritic alloy. *Scr. Metall. Mater.* **1993**, *29*, 479–484. [[CrossRef](#)]
24. Tomita, M.; Inaguma, T.; Sakamoto, H.; Ushioda, K. Development of Recrystallization Texture in Severely Cold-rolled Pure Iron. *ISIJ Int.* **2016**, *56*, 693–699. [[CrossRef](#)]

